Magnetic resonance induced heating of implantable leads

Michele Triventi[a], Eugenio Mattei[a], Giovanni Calcagnini[a], Federica Censi[a], Pietro Bartolini[a], Wolfgang Kainz[b] and Howard Bassen[b]

[a] *Dipartimento di Tecnologie e Salute, Istituto Superiore di Sanità, Rome, Italy*

[b] *Center for Devices and Radiological Health, Food and Drug Administration, Rockville, MD, USA*

Summary. In this study a methodological approach for measuring temperature and local absorption rate (SAR) on thin metallic structures, such as pacemaker (PM) leads, is provided. First preliminary experiments were performed to evaluate the error in temperature and SAR measurements made by fluoroptic® temperature probes when the temperature probe is in different contact configuration with the PM lead tip. Our results show how the position of temperature probes affects the temperature and SAR value measured at the lead tip. The transversal contact between the thermal sensor and the lead tip is the configuration which leads to the highest values for temperature and SAR. In the second part of this paper we describe two physical models of a human trunk and an experimental set-up to investigate the influence of the implant geometry and of the lead path on the heating and the local SAR deposition. Experiments reveled that the implant location and configuration are crucial elements for the heat generation at the lead tip.

Key words: magnetic resonance imaging, pacemaker, artificial, heating, electromagnetic energy, fluorescent probes.

Riassunto *(Riscaldamento prodotto su cateteri metallici impiantati durante risonanza magnetica)*. Nel presente contributo viene in primo luogo proposto un metodo di misura per temperatura e potenza depositata (*specific absorption rate*, SAR) su strutture metalliche sottili, quali un elettrocatetere di un pacemaker, utilizzando sonde a fluorescenza in fibra ottica. A tal fine, un primo gruppo di prove sperimentali è stato dedicato alla valutazione dell'errore che si compie sulle misure di temperatura e SAR in funzione della posizione che le sonde a fibra ottica occupano nell'intorno dalla punta dell'elettrocatetere. I risultati ottenuti mostrano come il posizionamento delle sonde influenzi in significativamente il valore di temperatura misurato: il contatto trasversale tra il sensore termico e l'elettrodo di stimolazione è la configurazione che permette di misurare il più alto valore di temperatura e SAR. Nella seconda parte del lavoro sono descritti due modelli fisici di simulatori di tronco assieme ad un *set-up* sperimentale utilizzato per studiare il contributo dato al riscaldamento dalla geometria e dal percorso compito dall'elettrocatetere. Le prove condotte dimostrano come il posizionamento e la configurazione dell'impianto siano elementi discriminati per il riscaldamento prodotto sulla punta dell'elettrocatetere.

Parole chiave: imaging a risonanza magnetica, pacemaker artificiale, riscaldamento, energia elettromagnetica, sonde a fluorescenza.

INTRODUCTION

Magnetic resonance imaging (MRI) is a widely accepted tool for the diagnosis of a variety of disease states. However, the presence of a metallic implant, such as a cardiac pacemaker, or the use of conductive structures in interventional therapy, such as guide wires or catheters, are currently considered a strong contraindication to MRI [1-4]. Potential effects of MRI on pacemakers (PM), implantable cardioverter defibrillators (ICD) and other active implantable medical devices (AIMD) include: force and torque effects on the pacemaker [5, 6]; undefined reed-switch state within the static magnetic field [7]; potential risk of heart stimulation and inappropriate pacing [8, 9] and heating effects at the lead tip [10-12]. In particular, most of the publications dealing with novel MR techniques on patients with implanted linear conductive structures [13-17] point out that the presence of these structures may produce an increase in power deposition around the wire or the catheter. Unfortunately, this increased local absorption rate (SAR) is potentially harmful to the patient due to possible excessive temperature increase which can bring living tissues to necrosis. The amount of heating has been investigated by several groups and temperature elevations observed spread from not significant values up to tens of degrees. For example, Achenbach *et al.* [10] reported a temperature increase of 63.1 °C for a PM lead; Rezai *et al.* [18], observed 25.3 °C at the end of a

Indirizzo per la corrispondenza (Address for correspondence): Michele Triventi, Dipartimento di Tecnologie e Salute, Istituto Superiore di Sanità, Viale Regina Elena 299, 00161 Rome, Italy. E-mail: michele.triventi@iss.it.

deep brain stimulation electrode; Roguin *et al.* [19] reported a maximum increase of 5.7 °C at 3.54 W kg^{-1} whole body specific absorption rate (WB-SAR). Sommers *et al.* [11] with a WB-SAR of 1.3 W kg^{-1} obtained temperature increase ranging from 0.1 to 23.5 °C, depending on the electrode type. Also some numerical approaches have been attempted: Irnich *et al.* [20] calculated the electric field distribution around a lead tip as function of the distance from the electrode surface and assessed that the sharp decrease of the power density could not cause any significant histological damage on living tissue, even with pretty high electrode temperature rise.

To date, as many as 10 deaths have been attributed to MRI procedures in patients with PM [21]. However, during clinical investigations and physician-supervised MRI procedures, some studies report no adverse events, suggesting that the presence of a permanent PM may no longer represent a strict contraindication to MRI [22].

Several factors influence the degree of heating: 1) the WB-SAR has been shown to correlate to the temperature increase [17], 2) the cooling effect of the blood around the leads is often not quantified, 3) the length and the geometric structure of the lead and 4) the implant location as well as the lead path. In addition, since thin linear structures such as PM leads may generate temperature gradients which can not be neglected with respect to the physical dimension of temperature probes, also the relative positioning of the temperature probe and the lead tip may significantly affect the measurement and can explain, at least partially, the inconsistency of the results in literature.

This paper describes two physical models of a human trunk and an experimental set-up to investigate the role of the implant geometry to the heating and the local SAR deposition. An estimation of the temperature and SAR measurement error made by using Fluoroptic® temperature probes is also provided. In addition, for a given whole body SAR, we compared the temperature increases induced by a real MRI scanner to those obtained in a MR coil simulator, in order to understand whether the whole body averaged SAR calculated by a clinical MRI system can be used as a reliable metric for radiofrequency (RF) induced heating or not.

MATERIALS AND METHODS

We used three different experimental set-ups: in the first one, we performed temperature measurements on the tip of a PM lead inside a rectangular box phantom, using different types of contact positions between the probe and the lead tip. In this preliminary configuration, the heating was obtained by injecting into the lead a RF current which flowed through the lossy-gelled material the phantom was filled with. Then, we placed inside the same rectangular box a PM can with its leads and measured the temperature increase inside a MR birdcage coil *(Figure 1a)*. The third experimental set-up was a human-shaped phantom implanted with a PM and its leads, placed inside a real clinical MRI scanner *(Figure 1d)*.

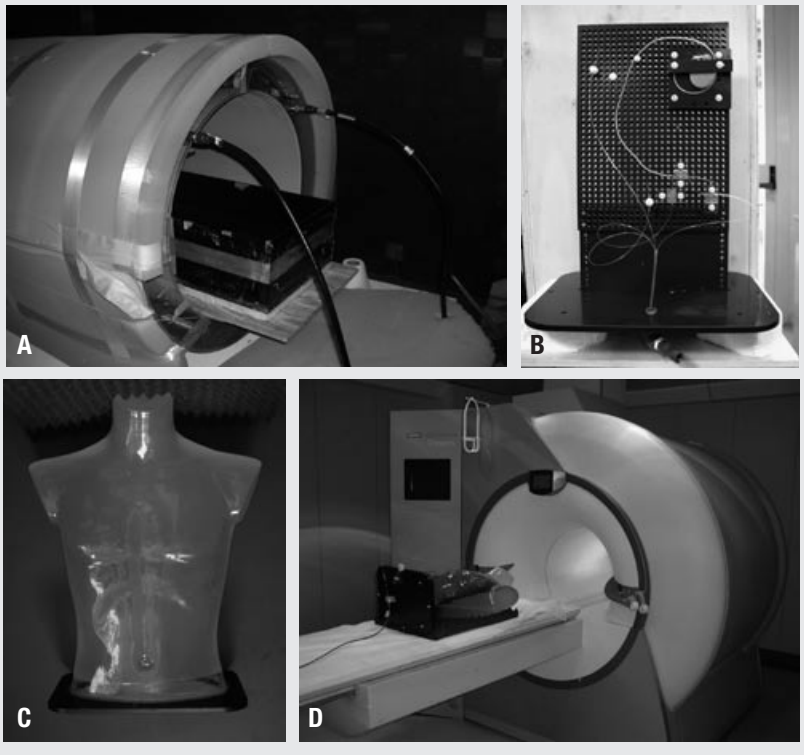

Fig. 1 | *Pictures of the MRI birdcage coil used for the rectangular box phantom (a); the PVC grid which supports the pacemaker implant and the Fluoroptic® temperature probes (b); the human-shaped phantom (c) filled with the HEC gel and used in a clinical MRI scanner (d).*

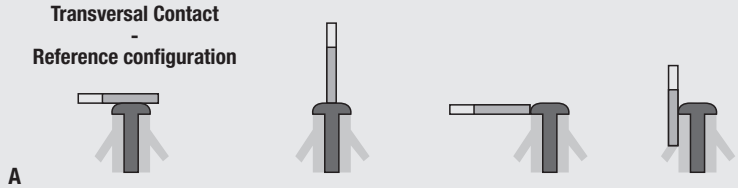

A

Contact configuration	Tip-to-side	Tip-to-tip	Side-to-side
25 MHz	-39%	-35%	-34%
64 MHz	-36%	-32%	-28%
128 MHz	-7%	-6%	-4%

B

Contact configuration	Tip-to-side	Tip-to-tip	Side-to-side
25 MHz	-72%	-75%	-68%
64 MHz	-65%	-65%	-48%
128 MHz	-30%	-20%	-15%

Fig. 2 | *Comparison among measurements obtained with the electrode of the pacemaker lead in transversal contact with the pigmented part of the Fluoroptic® probe (reference) and underestimation obtained with other contact configurations: temperature (a) and SAR (b) comparison. A schematic representation of each contact configuration we tested is also reported in the upper panel of the figure.*

In our experiments, we used a dual chambers PM (Elect D, Sorin Biomedica CRM, Italy) and a biventricular PM (three chambers, NewLiving CHF, Sorin Biomedica CRM, Italy), with both unipolar and bipolar leads (mod. S80T and S80TB, Sorin Biomedica CRM, Italy). Lead length was 62 cm, tip area 6 mm^2, and ring area 36 mm^2. Both the rectangular box and the human shaped phantom were filled with 2% hydroxy-ethyl-cellulose (HEC), 0.36% sodium chloride and the rest water: a gel saline solution with 0.59 Sm^{-1} conductivity and 79 permittivity at 64 MHz, and 4178.3 J $kg^{-1}K^{-1}$ heat capacity [23].

Because of the well-known limitations of conventional thermometry methods in radio frequency (RF) energy environments [24, 25], we used a Fluoroptic® thermometry (Luxtron, Model 3100, USA – SMM probes), with resolution of 0.1 °C, operating at 8 samples per second. This method has become the "state-of-the-art" and the industry standard in temperature and SAR evaluation inside MRI system and has been used to examine radiofrequency energy-induced heating of tissues, *in vitro* and *in vivo* [25-29]. In such probes, the temperature sensor is a half-sphere of approximately a 0.3 mm diameter encapsulated inside a cylindrical pigmented jacket and located at the terminal portion of a flexible fiber optic cable. The pigmented jacket (approx. 3 mm length, 0.8 mm diameter) has to prevent ambient light from interfering with the sensor, as well as acts as a reference for the probe positioning.

With the experimental data obtained from the Fluoroptic® probes we estimated the local SAR by calculating the slope (dT/dt) of the initial temperature increase. This slope was estimated by minimizing the least square error over about 40 samples; the estimation was assumed valid when the Pearson coefficient r^2 was greater than 0.98 [30].

Probe positioning

Our first experiment was aimed to identify the optimal contact configuration between the temperature probe and the lead tip, in order to minimize the underestimation related to temperature measurements. To investigate how the position of the pigmented region of the probe affects the temperature measured on a PM lead tip, we used a PVC box (a 28 × 20 × 26 cm box) filled with the gel described above. A 26 × 18 cm grid was submerged in the gel to support the pacemaker and its lead and maintained a consistent separation distance between the implant, phantom gel surface and the temperature probes. The grid was adjusted so that the top of the implant was positioned below the phantom surface. SAR and temperature were measured on the tip a unipolar lead. A RF signal was injected into the lead using a coaxial cable connected to the lead. The outer conductor (signal ground) was connected to a 1 × 20 × 10 mm silver plate located on one side of the PVC box. The current through the gel went from the lead tip to the silver plate. The lead was placed in the gel 5 cm below the phantom top surface, simulating an implant in the human body. The distance between the silver plate and the lead tip was 7 cm. Three sinusoidal excitations were studied: 25, 64 and 128 MHz, which approximately correspond to the RF field used in 0.5, 1.5, and 3 T MRI systems. The signals were generated by a RF generator (Rhode & Schwartz – SMT 06), and then amplified (RFPA – RF 06100-6, France); a power meter (Rhode & Schwartz – NRT Z14) connected to the output of the amplifier measured the average net-input power to the lead.

The preliminary measurements investigated various contact configurations between the terminal part of the temperature probes and the pacing electrode at the lead tip. Aim was to identify the temperature probe position which results in the maximum temperature result and to assess the relative underestimations associated with other configurations.

We studied the following possibilities *(Figure 2)*:

a) transversal contact between the side of the temperature probe and the circular surface of the lead tip;

b) transversal contact between the tip of the temperature probe and the side surface of the electrode;
c) axial contact between the tip of the temperature probe and the circular surface of the lead tip;
d) axial contact between the tip of the temperature probe and the side surface of the electrode.

The underestimation was expressed as the percentage difference of the temperature increase measured with the particular temperature probe position in respect to the position leading to the maximum temperature measurement.

Rectangular phantom

Once we identified the temperature probe position which results in the maximum heating, we used it to perform several measures on a PM can and PM lead tip, inside a MR birdcage coil *(Figure 1a)*. These measurements were performed at the Center for Device and Radiological Health (CDRH), Food and Drug Administration (FDA) in Rockville, MD, USA. The birdcage coil was housed in an anechoic chamber and fed in quadrature sinusoidal excitation by a signal generator (HP8647A, USA) connected to a 150 W 64 MHz RF amplifier. The output power was continuously monitored by a directional coupler and a power meter (HP436A, USA). In this configuration, we used the same rectangular box phantom described in the previous section, and the RF energy (~100 W) delivered to the box corresponded to a WB-SAR of about 1.0 W kg^{-1}. Also the position of the grid did not change. The PM (dual chambers and biventricular) was mounted on the grid and programmed either in sensing or pacing mode. We tested both unipolar and bipolar leads and no more than two leads were tested simultaneously.

First goal of these measurements was to evaluate the contribution to the lead tip heating from the area covered by the implant. In our experiments, the total area of the implant was varied by wrapping the exceeding lead near the PM body or by changing the lead geometry. An example of varying the lead geometry is shown in *Figure 3a*, when the lead is placed in loops around the PM can. Different areas of the implant were also obtained by keeping the position of the PM can and the lead tip constant and varying the lead path. For each configuration we computed the total area of the implant, defined as the region delimited by the lead itself, the PM can and the line connecting from lead tip to the center of PM can (*Figure 3a*, shaded areas). In this series of experiments, the PM was always positioned as a

a

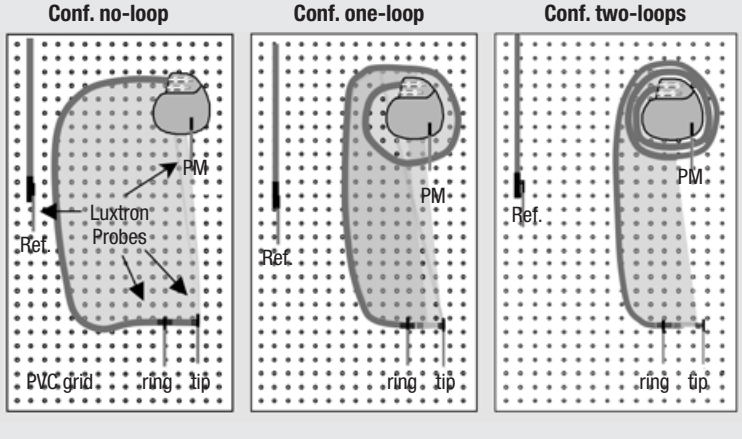

b

Implant area (cm^2)	PM Configuration	Temperature increase (°C)	SAR (W kg^{-1})
280	No loop	7.3	2100
270	No loop	11.9	3000
225	No loop	10.5	2565
150	No loop	2.0	500
210	One loop	5.8	1500
180	One loop	4.0	1250
150	One loop	2.1	600
120	One loop	1.8	480
115	Two loops	0.4	60
90	Two loops	0.2	40
70	Two loops	0.5	80
65	Two loops	0.9	180

Fig. 3 | *Examples of implant configurations tested in the MRI simulator: no loop, one loop and two loops configurations (a). The position of the optical probes and of the wire used as reference is also illustrated. (b) Values of temperature increase and SAR measured during the experiments with the rectangular box simulator, reported in function of the implant area and configuration. Different implant areas were obtained either by wrapping the lead around the PM body and by changing the lead path.*

Table 1 | *Main parameters of the MRI clinical sequences used during the human-shaped phantom experiments. In the last columns of the table the two time length used for each type of sequence are reported*

Sequence type	Siemens sequence name	TR (ms)	TE (ms)	Flip angle	Length of long sequences (s)	Length of short sequences (s)
Single shot (turbo fast) spin echo	HASTE	1190	83	150	402	42
Steady state free process	TrueFISP	3.78	1.89	54	379	38
Spoiled gradient echo	FLASH	960	40	20	417	53

left sided implant and the main vertical segment of the lead was always to stay in the central portion of the rectangular phantom.

We then focused on the position of the implant inside the gelled material: different lead geometries were tested, with the main straight segment in one experiment close to the edge, whereas in the other centered in the phantom. The dual chambers PM allowed investigating two different lead geometries at the same time. Great care was taken to maintain a consistent separation distance between the tips to avoid interactions between the two lead tips. Temperature was measured by Fluoroptic® probes at the lead tips and at the PM can. In case of bipolar lead, a probe was positioned in transversal contact with the ring at the lead. Moreover, the temperature increase was also measured at the terminal part of an insulated metallic wire, which was placed always in the same position on the grid, far from the PM and its leads. This value was used as a reference for data acquired in different experiments.

Each experiment consisted in a base measurement of about 60 seconds, followed by an exposure to RF lasting 200 seconds. Also the cooling phase after RF exposure was recorded for a period of 200 seconds.

The acquisition system was made of an analog-digital converter connected to the output of the Fluoroptic® thermometer and to a 16-bit acquisition card (DAQCard-AI-16XE-50 – National Instruments) boarded on a personal computer, where the temperature changes were displayed in real time.

Human-shaped phantom

In order to simulate physiological implant configuration and realistic MRI procedures, further experiments were performed in real MRI scanning system using a human-shaped torso simulator developed at the Department of Technology and Health of the National Institute of Health (Istituto Superiore di Sanità, ISS) in Rome *(Figure 1c)*. The simulator consists of a torso-shaped transparent PVC phantom of the size of a 70 kg male. Internal volume of the torso is 32 liters [23]. A PVC grid is mounted inside the torso to support a dual chambers PM connected to two bipolar leads, and the temperature probes. The torso was filled with the same gel as described above.

The actual lead geometry and PM placement can vary from patient to patient. The PM can be located in the left or right pectoral region. Since the length of the lead may not fit the patient's anatomy and size, the exceeded length is usually wrapped near or around the PM can. Our experiments were performed on a siemens magnetom sonata maestro class scanner (1.5 Tesla) *(Figure 1d)*. Three different RF sequences commonly used in clinical MRI procedures with two different sequence lengths each were tested. The main parameters of the sequences are summarized in *Table 1*. The MRI parameters (TR, TE and Flip Angle) were adjusted to reach a WB-SAR of 2 W kg^{-1}, as estimated by the scanner. The geometry of the implant reproduced left and right PM placements. For each implant, three lead paths were tested: without lead looped around the PM (no-loop configuration) and with the lead forming one or two loops around the PM (1-loop configuration and 2-loops configuration, respectively). For each lead path, the length and the position of the linear section of the lead as well as the lead tip position were kept constant. Only the PM was moved from the left to the right pectoral location.

Temperature was recorded during the time when the RF excitation was on and in the following cooling period, for about 60 s. The Fluoroptic® probes were positioned at the lead tips, on the PM can and in the gel, far from metallic structure, as reference.

RESULTS

Probe positioning

In *Figure 2* we reported the differences in temperature and SAR measurements at the peacemaker lead tip due to different contact configurations with the Fluoroptic® probes. At the three frequencies we tested (25 MHz, 64 MHz and 128 MHz) we used an average net power of 0.7 W, 1.36 W and 2.04 W, respectively. These power levels were chosen to obtain heating comparable to those reported in the literature [1, 3, 13, 14]. We found that the position of the temperature probe significantly affects the measurement: transversal contact between the side of the temperature probe and the circular surface of the lead tip is the configuration which leads to the highest measured temperature. We define the temperature measured with other positions than the one leading to the maximum value as an underestimation *(Figure 2)*.

The highest temperature underestimation occurred at 25 MHz and it decreases as the frequency increases, regardless of the temperature probe contact. The configurations "tip-to-side" and "tip-to-tip" result-

ed in temperature underestimations ranging from 28% to 39%. The underestimation associated with the side-to-side contact was significantly lower (4% - 7%).

The underestimation associated with the measurement of local SAR at the lead tip showed a similar behavior: transversal contact between the side of the temperature probe and the circular surface of the lead tip is the configuration measuring the highest SAR (1444 W kg^{-1}). The underestimation associated with other temperature probe configurations is reported in *figure 2b*. In the worst case, the SAR underestimation can be up to 75%. The effect of the frequency on SAR underestimation was similar to that observed for the temperature.

More details about the error associate to temperature and SAR measures using Fluoroptic® probes in contact with thin metallic structures can be found in [31].

Rectangular phantom

The major increase of temperature was always observed at the lead tip. No significant increase of temperature was observed at the PM can and no differences were observed between the two PM models (dual chambers and biventricular). The ring electrode of bipolar leads showed much lower temperature increase than the tip. We did not observe any significant difference in the tip temperature between unipolar and bipolar leads, as well as changing the programming of the PM from unipolar to bipolar sensing/pacing. When the PM was connected to multiple leads simultaneously, we did not observe significant changes in the amount of heating of each tip, if consistently separated, respect to the single lead configuration.

Figure 3b shows the temperature increase at the lead tip, for various implant areas. In *Figure 3c*, SAR values at the lead tip, for the same experiments, are plotted as a function of the implant area. As the area increases, we observed a temperature increase and a local SAR increase. Note that the different areas were obtained either by wrapping the exceeded lead near the PM body or by changing the lead path.

The increase of temperature and SAR at the lead tip seems to be directly related to the implant area. The lead around the PM body or the number of loops does not seem to play a significant role. Configuration with no-loop and one-loop, but approximately sharing the same areas, produced simi-

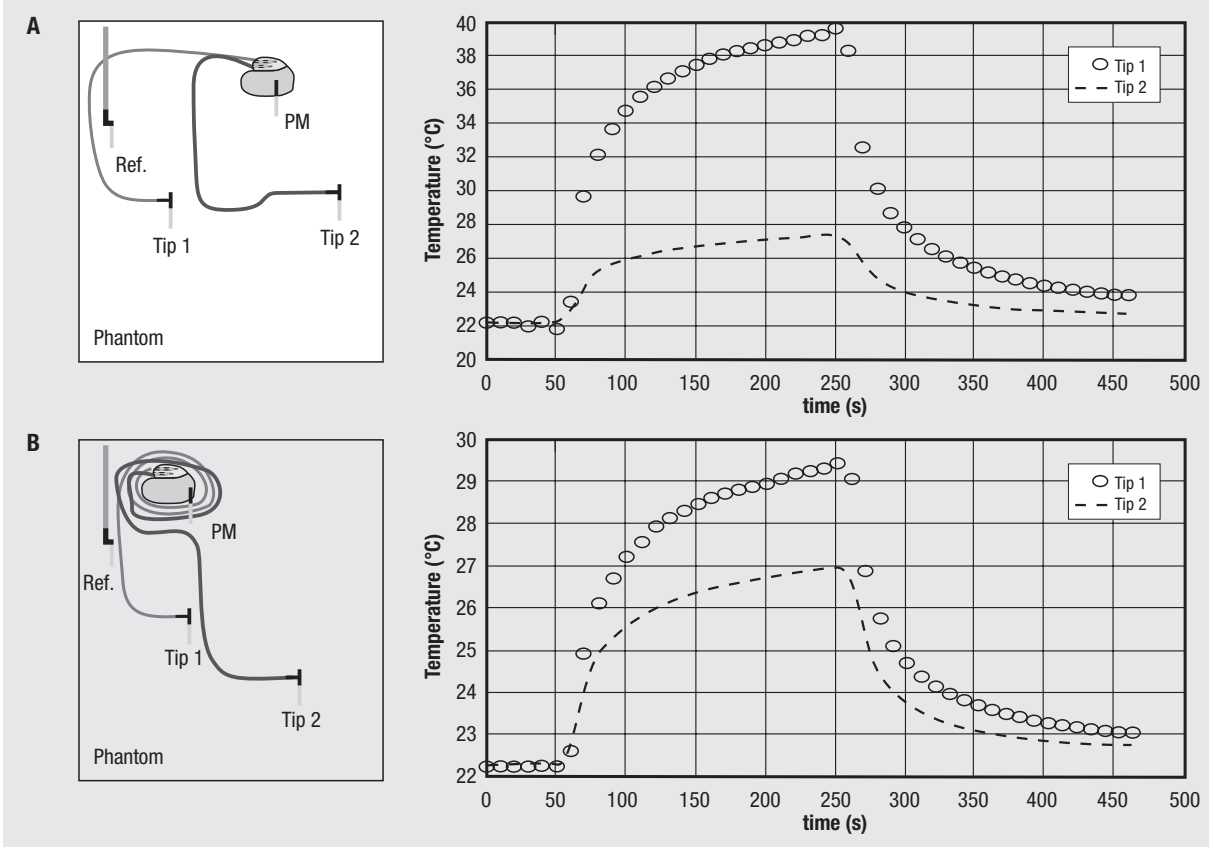

Fig. 4 | *Examples of temperature increases measured in the rectangular box phantom: comparison between two configurations with the same implant area but different position inside the box (a); comparison between an implant with a larger area but in the centre of the phantom and an implant with a smaller area but placed close to the edge of the box (b). The position of the optical probes and of the wire used as reference is also illustrated.*

Table 2 | *Temperature increase (°C) and lead tip SAR (W kg-1) of human-shaped phantom experiments. Average whole body SAR calculated by the scanner is also reported. The data refer to long MRI sequences*

Sequence	Left pectoral implant			SAR* (W kg^{-1})	Right pectoral implant			SAR* (W kg^{-1})
	No loop	*1-loop*	*2-loops*		No loop	1-loop	2-loops	
HASTE	6.3 (1362)	0.9 (-)	0.7 (-)	1.70	11.9 (2345)	2.68 (641)	1.0 (-)	1.72
TruFISP	6.2 (1255)	1.0 (-)	0.6 (-)	1.70	12.3 (2375)	2.5 (536)	1.0 (-)	1.70
FLASH	0.1 (-)	< 0.1 (-)	< 0.1 (-)	0.02	< 0.1 (-)	< 0.1 (-)	< 0.1 (-)	0.02

**SAR: average whole body specific absorption rate computed by the scanner; (-): SAR not estimable, due to low temperature increase..*

lar temperature increase local and SAR. Two experiments showed temperature increase (and SAR values) significantly higher then what expected from their implant area. A retrospective analysis of these configurations showed that the lead had a relatively long straight path (approximately 20 cm).

The position of the implant inside the phantom seemed to be even more important than the implant area. *Figure 4a* shows the temperature increase for two leads with a pretty similar geometry but with their main vertical segment in different regions inside the phantom: the lead along the edge of the box produced a significant higher heating at its tip than the one placed in the central region. Even when the implant in the middle of the phantom covered a larger area that the one close to the edge of the box (1-loop *vs* 2-loop configuration), the temperature increase is higher if the lead is aligned along the edge of the box *(Figure 4b)*.

In all our experiments, the temperature measured by the probe not in contact with the wire used as reference did not change significantly. It gives good consistency and reproducibility to the measures.

Human-shaped phantom

The temperature increase and local SAR values for the experiments using a real MRI scanner are reported in *Table 2*. As for the clinical sequences, the gradient echo (Flash) did not induce detectable temperature increase (below the Luxtron probe sensitivity, 0.1 °C) in all the configurations tested. Scanning sequences with as relatively high whole body SAR, led to a temperature increase up to 12.3 °C. For left pectoral PMs the lead area appears to be the major factor relevant for the heating. A high implant area (no loop) showed always a higher temperature increase than the 1-loop and 2-loops configurations.

Surprisingly, when the PM is right pectoral implanted, the lead position seems to play the major role: the vertical segment of the leads did not change for the two implant configurations, whereas the initial horizontal parts were placed on opposite sides on the grid *(Figure 5)*. No-loop configurations showed always a temperature increases significantly greater then the 1- and 2-loops configurations. In addition, the temperature increase observed were even greater then those of the left implants. In both configurations (left and right) the temperature increase and local SAR were proportional to the whole body SAR reported by the scanner.

The data reported in *Table 2* refer to long sequences; the comparison between short and long sequences showed that, as observed during continuous wave exposition in the rectangular box simulator, the major temperature increase occurred within the first minute. Experiments were repeated changing MRI parameters such as the center of view (chest, abdomen and pelvis) and the field of view (200, 300 and 400 mm) without significant changes in the heating.

In all experiments no significant temperature increase was observed in the gel, far from the PM and its leads, for all the sequences we tested.

DISCUSSIONS

Previous studies investigating MRI induced PM lead heating reported a large variability in the induced heating. All investigations showed that the maximum RF-induced heating occurs at the electrode tip. However, the reported temperature increase at the lead tip varied between 0.1 °C [11] and 63.1 °C [10]. This variability comes from several factors, such as the type and positioning of the temperature probes next to the lead tip, the whole body SAR used, the cooling effect of the blood flow, and the lead geometry and placement.

The aim of this paper was first to identify a positioning of temperature probes next to PM lead tips to measure the maximum lead tip heating. Then we investigated the effect of the geometric structure of the PM leads (lead geometry) and the placement of the pacemaker on the PM can heating and PM lead tip heating, induced by MRI.

Using temperature measurements on a physical model of a pacemaker lead we found that the positioning of the temperature probes strongly affects the temperature and SAR results. Due to the comparable dimension of the temperature probes with

the pacing electrode and due to the large spatial temperature gradient around the lead tip, temperature probes tend systematically to underestimate the real value of local temperature and SAR. In particular, using the SMM Luxtron fluoroptic® probes, we found that a transversal contact of the temperature probe with the lead tip always gives the highest temperature and SAR values. Such a result points out that the active sensor is likely to occupy the central region of the pigmented jacket of the temperature probe. Assuming this configuration as reference, the underestimation by other configurations may be as high as 39% for temperature and 75% for SAR. Furthermore, we found less underestimation as the frequency increases. We can speculate that the heating pattern at higher frequencies is more spread and thus the effect of probe size and positioning is less marked. A deeper analysis of this issue was beyond

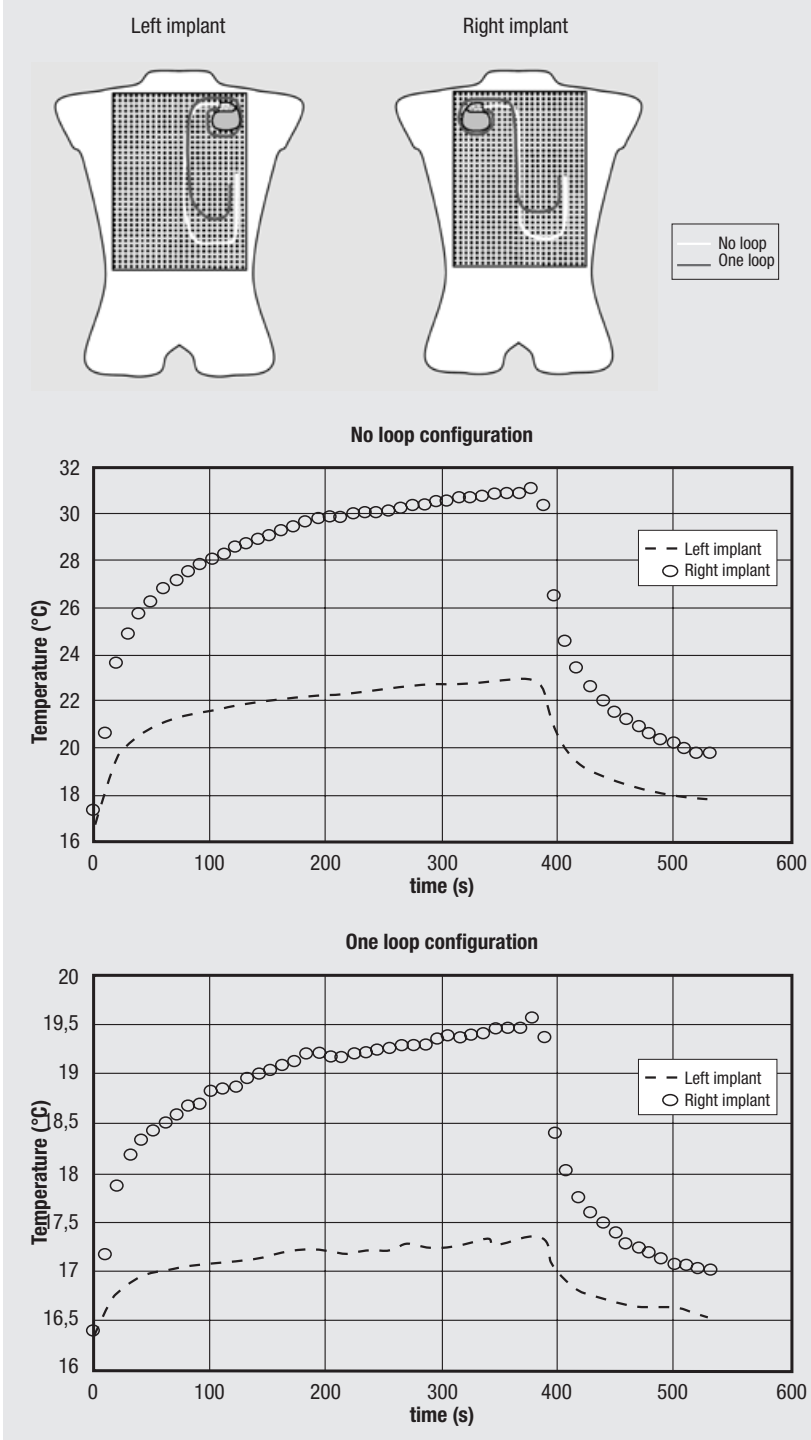

Fig. 5 | *Sketches of the two implant configurations tested in a real MRI scanner using the human-shaped phantom and graphs of the temperature increase measured at the lead tip: no loop and one loop configurations for both left and right pectoral implants.*

the aim of this study. The investigation of the temperature and SAR errors from other Fluoroptic® probe types, such as surface and remote style probes, was also beyond the aim of this study. Additional experiments are needed to evaluate the usability of surface and remote style probes for MRI implant heating evaluations. The SMM probes were chosen because they can guarantee a reliable contact even with very thin wires. In addition, since heating is generated at the interface between the metallic structure and the gel, surface contact probes would not be located in the actual hot spot area.

Experiments in the rectangular box phantom revealed two major factors on the lead tip heating: the length of the straight segment of the lead and their position inside the phantom. At first we correlated the heating induced by a MRI exposure to the area covered by the implant: several papers in the literature [11, 19] chose a configuration of the pacemaker lead in the coronal plane to achieve a maximal magnetic induction area, in order to maximize the heating at the lead tip. Our data clearly shows that the temperature increase is proportional to the implant area. Interestingly, in some cases, similar areas gave different temperature increase. It suggests that the lead tip heating is more affected by the length of the straight lead segment than the area. Generally a larger area implies a longer straight lead segment, as it happens for the no-loop, 1-loop and 2-loops configurations.

Resonance phenomena in various kinds of linear metallic leads and wires (*e.g.*, catheters used in interventional radiology) have been hypothesized by various groups [32, 33]. From a theoretical point of view, the maximum electrical coupling occurs when the length of a linear wire is half the wavelength of the RF field. At 64 MHz, the critical length of a straight lead implanted in the human body is around 26 cm [33]. This value is close to the length of the linear section of the lead in the experiments where the highest temperature increase and SAR values were observed.

The position of the implant inside the phantom seems to play a major role in the heat generation process. When the lead is placed close to the edge of the phantom, the temperature increase at the tip is significantly higher than for implants of the same area, or even larger, but positioned in the central region of the box. The electric field generated by the MR coil is higher at the phantom's edges, which represent a discontinuity between air and a lossy material, such as the HEC gel. The electric field sharply decreases towards the centre of the phantom. The inducted currents generated inside the simulator by the magnetic field are as well confined along the border of the box. In conclusion, we can define an implant configuration with long straight lead segments close to edge of the phantom to maximize the lead tip heating.

In our experiments using the rectangular box phantom, we kept the position of the PM can constant, simulating a left implant configuration. That is the most common situation for a real pacemaker. The results obtained for a left implanted PM inside the human shaped phantom were consistent with those obtained by the rectangular box: the longer the vertical segment of the lead, the higher the temperature increase. The importance of the position of the lead inside the phantom rather than the area of the implant is once again highlighted by the results from the right-implant configurations: they showed smaller lead areas than left pectoral implanted PMs, but the temperature increase observed were higher. In the two implant configurations, the vertical segment of the lead did not change, whereas only the PM can and the initial horizontal parts of the lead were placed on opposite sides on the grid. This suggests that the magnetically induced voltage could either add to or subtract from the voltage generated by coupling with the electrical component of the RF field to the linear part of lead [18]. The higher temperature increase for right-pectoral implants may also come from an asymmetric distribution of the electromagnetic field inside the phantom, with a "hot spot" area in the upper-right region of the torso simulator.

For approximately 1 W kg^{-1} WB-SAR we observed, in worst case, 12 °C lead tip heating and local SAR up to 2300 W kg^{-1}. The *in vitro* test methods used here are not intended to simulate the dynamics of blood and body fluid, but rather simulate the nearly instantaneous energy deposition. Thus, in a patient the temperature elevation may be reduced by the surrounding tissue heat absorption. Moreover, the power density at the lead tip decreases very sharply as the distance from the electrode increases: Irnich *et al.* [20] developed a numerical model for the evaluation of the electric field distribution around the lead tip and they found that a temperature increase of 80 °C was necessary to achieve a 5 °C degree heating 1 mm away from the electrode's surface. This could be true if the SAR were the only determinant for the thermodynamic equilibrium, neglecting any conductive processes from the hot spot to the surroundings tissues. Actually, our results suggest that the lead tip heating caused due to MRI exposure may damage, in particular configurations, biological tissue or at least may cause an alteration of the contact impedance at the tip, compromising the pacing capability.

The major impact of the implant positioning inside the phantom implies the need to perform temperature and SAR measurements inside a realistic human shaped trunk simulator, so to reproduce a realistic and worst case distribution of the inducted current inside the phantom.

Both the rectangular box and the human-shaped phantom measurements showed that wrapping the exceeding lead near the PM can does not contribute to the heating. We either observed that unipolar and bipolar leads produced similar heating and that no significant temperature increase was measured on the PM can. For bipolar leads we measured the temperature also at the ring electrode and found

little temperature increase (less than 2 °C). Similar results were found by other groups, even with different types of heating sources [34]. Due to the larger surface area of the ring electrode compared to the lead tip, the current density, and therefore the temperature increase, is much lower than at the tip.

We also explored if other PM settings influence the lead tip heating. We found that the lead tip heating is independent of the PM programming (*e.g.*, unipolar/bipolar sensing and pacing). Particularly we found no significant difference between bipolar to unipolar leads. The simultaneous use of two or three leads does not change systematically the heating of each tip, even when the tips are close to each other. However, a certain temperature increase with respect to the single lead configuration may happen.

The measurements inside the real MRI scanner showed that also the RF excitation sequence is a discriminating factor for the lead tip heating: in particular, the gradient echo sequences did not cause a significant temperature increase any of the implant configurations we tested.

Baker *et al.* [17] demonstrated that the whole body averaged SAR calculated by different MRI systems is not a reliable metric for RF induced heating. They found that in one system a WB-SAR of 0.07 W kg^{-1} induced temperature increase of 8.4 °C, while the same implant had a temperature increase of 1.2 °C with a WB-SAR of 0.88 in a different MRI system from the same manufacturer. We found similar differences when we tried to compare, for a given WB-SAR, the heating found in the rectangular torso simulator with a real MRI system. Using the rectangular box phantom (WB-SAR 1.0 W kg^{-1}) we obtained for a given lead configuration a temperature increase of about 12 °C. The same configuration gave in a real MRI system a temperature increase of about 6 °C for a SAR of 1.70 W kg^{-1}. We assume that this difference is due to an overestimation of the WB-SAR by the real MRI system. In this case the real MRI system overestimates the WB-SAR by a factor of 3.4. Such a WB-SAR overestimation leads to the same factor of underestimation for the implant heating because most testing of implant heating relates the temperature increase to the whole WB-SAR given by the MR system (M-WB-SAR). This may be due to the use of different assumptions and algorithms by the MR systems and due to the fact that the estimation by the scanner might not be valid for phantoms. In phantoms the M-WB-SAR estimation (M-WB-SAR-P) can be verified using calorimetry (C-WB-SAR-P) whereas in humans the M-WB-SAR estimation (M-WB-SAR-H) can only be verified using computational methods and high resolution anatomical models or the power per pulse method (C-WB-SAR-H). For implant heating evaluations the question comes up what relation between M-WB-SAR-H, C-WB-SAR-H, M-WB-SAR-P, and C-WB-SAR-P gives a conservative and therefore safe estimation of the actual implant heating in a patient. For implant heating evaluations an ideal relation between the WB-SAR values for humans and phantoms would be:

$$\text{M-WB-SAR-H} = \text{C-WB-SAR-H} \quad (1)$$

$$\text{M-WB-SAR-P} = \text{C-WB-SAR-P} \quad (2)$$

However, for patient safety the M-WB-SAR-H value is usually a conservative estimation of the C-WB-SAR-H:

$$\text{M-WB-SAR-H} \geq \text{C-WB-SAR-H} \quad (3)$$

Manufacturers of MR systems indicate that the WB-SAR estimation of the machine is not valid for phantoms. An M-WB-SAR-P overestimation leads to an underestimation of the same factor for the reported implant heating. This does not necessarily pose a problem for implant heating evaluations if the overestimation for M-WB-SAR-H is the same as for M-WB-SAR-P:

$$\frac{\text{M-WB-SAR-H}}{\text{C-WB-SAR-H}} = \frac{\text{M-WB-SAR-P}}{\text{C-WB-SAR-P}} \quad (4)$$

the actual implant heating occurring in the patient at a certain M-WB-SAR-H level would be correctly predicted. Also, as long as the overestimation of the WB-SAR for humans (M-WB-SAR-H) is greater than the overestimation for the phantom the implant heating evaluation can be considered as conservative:

$$\frac{\text{M-WB-SAR-H}}{\text{C-WB-SAR-H}} \geq \frac{\text{M-WB-SAR-P}}{\text{C-WB-SAR-P}} \quad (5)$$

Inequality (5) must be true for all humans to ensure patient safety. For safety considerations a conservative approach is desirable which has to assume that the C-WB-SAR-H can reach the M-WB-SAR-H in a worst case patient:

$$\frac{\text{WB-SAR-H}}{\text{WB-SAR-H}} = 1 \quad (6)$$

Assuming (6) as the worst case for implant heating it can be followed:

$$\text{M-WB-SAR-P} \leq \text{C-WB-SAR-P} \quad (7)$$

Inequality (7) states that for conservative implant heating evaluations the M-WB-SAR-P must be an underestimation of the real SAR in the phantom (C-WB-SAR-P). Unfortunately this seems not to be the case. Our results indicate the M-WB-SAR-P is

also an overestimation of the true WB-SAR in the phantom (C-WB-SAR-P). Further research, comparisons and re-evaluations of WB-SAR estimation of real MR systems for humans and phantoms is urgently needed to resolve this problem.

CONCLUSIONS

Our experiments showed the sensitivity of temperature and SAR measurements on Fuoroptic® probe contact positioning. The transversal contact of the pigmented portion of the temperature probe and the lead tip minimized the underestimation for temperature and SAR and gave therefore always the highest values for this type of pacemaker lead. Other contact configurations may cause a temperature underestimation of up to 39% and a SAR underestimation of up to 75%. For all MRI heating evaluations with temperature probes, a contact position leading to the lowest maximum error should be used, and the error should be specified. Scientific sound MRI heating evaluations need to be accompanied by a thorough uncertainty budget. Therefore, other uncertainty factors should also be evaluated when specifying temperature and SAR values on implants based on measurements with Fluoroptic® temperature probes.

The results from the rectangular box and the human torso simulator showed that the lead tip heating during MRI exposure strongly depends on the implant geometry and its position inside the phantom. The maximum heating at the lead tip was found for a PM lead path with long straight segments close to the border of the phantom: in such a configuration, the temperature increase measured inside the MR birdcage coil for a WB-SAR of 1 W kg^{-1} was as high as 18 °C, with a local SAR of 4300 W kg^{-1}. In the human shaped phantom, more realistic implant configurations were reproduced: the maximum temperature increase was found for right implant configurations suggests that the magnetic-induced voltage could either add to, or subtract from the voltage generated by coupling of the electrical component of the RF field to the linear part of lead.

In conclusion, implant geometry and positioning inside the phantom has to be taken into account to understand the large variability of lead tip heating reported in the literature: lead paths with long straights segments close to the edge of the phantom have to be chosen to maximize the induced currents and the tip heating. In addition, the WB-SAR calculated by commercial MRI scanner is somehow correlated to the local heating, although it is not yet a reliable tool to estimate the hating and the local SAR at the lead tip.

Disclaimer

The opinions and conclusions stated in this paper are those of the authors and do not represent the official position of the Department of Health and Human Services. The mention of commercial products, their sources, or their use in connection with material reported herein is not to be construed as either an actual or implied endorsement of such products by the Department of Health and Human Services.

Submitted on invitation.
Accepted on 24 January 2007.

References

1. Niehaus M, Tebbenjohanns J. Electromagnetic interference in patients with implanted pacemakers or cardioverter-defibrillators. *Heart* 2001;86:246-8.
2. Pinski SL, Trohman RG. Interference in implanted cardiac devices, part II. *Pacing Clin Electrophysiol* 2002;25:1496-509.
3. Kanal E, Borgstede JP, Barkovich AJ, Bell C, Bradley WG, Etheridge S, Felmlee JP, Froelich JW, Hayden J, Kaminski EM, Lester JW Jr, Scoumis EA, Zaremba LA, Zinninger MD. American College of Radiology white paper on MR-safety. *Am J Roentgenol* 2002;178:1335-47.
4. Shellock FG, Crues JV III. MR-safety and the American College of Radiology white paper. *Am J Roentgenol* 2002;178:1349-52.
5. Luechinger R, Duru F, Scheidegger MB, Boesiger P, Candinas R. Force and torque effects of a 1.5-Tesla MRI scanner on cardiac pacemakers and ICDs. *Pacing Clin Electrophysiol* 2001;24:199-205.
6. Shellock FG, Tkach JA, Ruggieri PM, Masaryk TJ. Cardiac pacemakers, ICDs, and loop recorder: evaluation of translational attraction using conventional ("long-bore") and "short-bore" 1.5- and 3.0-Tesla MR systems. *J Cardiovasc Magn Reson* 2003;5:387-97.
7. Luechinger R, Duru F, Zeijlemaker VA, Scheidegger MB, Boesiger P, Candinas R. Pacemaker reed switch behavior in 0.5, 1.5, and 3.0 Tesla magnetic resonance imaging units: are reed switches always closed in strong magnetic fields? *Pacing Clin Electrophysiol* 2002;25:1419-23.
8. Erlebacher JA, Cahill PT, Pannizzo F, Knowles RJ. Effect of magnetic resonance imaging on DDD pacemakers. *Am J Cardiol* 1986;57:437-40.
9. Hayes DL, Holmes DR Jr, Gray JE. Effect of 1.5 tesla nuclear magnetic resonance imaging scanner on implanted permanent pacemakers. *J Am Coll Cardiol* 1987;10:782-6.
10. Achenbach S, Moshage W, Diem B, Bieberle T, Schibgilla V, Bachmann K. Effects of magnetic resonance imaging on cardiac pacemakers and electrodes *Am Heart J* 1997:134;467-73.
11. Sommer T, Vahlhaus C, Lauck G, von Smekal A, Reinke M, Hofer U, Block W, Traber F, Schneider C, Gieseke J, Jung W, Schild H. MR imaging and cardiac pacemakers: *in vitro* evaluation and *in vivo* studies in 51 patients at 0.5 T. *Radiology* 2000;215:869-79.
12. Luechinger R, Zeijlemaker VA, Pedersen EM, Mortensen P, Falk E, Duru F, Candinas R, Boesiger P. *In vivo* heating of pacemaker leads during magnetic resonance imaging. *Eur Heart J* 2005;26:376-83.
13. Dumoulin CL, Souza SP, Darrow RD. Real-time position monitoring of invasive devices using magnetic resonance. *Magn Reson Med* 1993;29:411-5.
14. Leung DA, Debatin JF, Wildermuth S, McKinnon GC, Holtz D, Dumoulin CL, Darrow RD, Hofmann E, von Schulthess GK. Intravascular MR tracking catheter: preliminary experimental evaluation. *Am J Roentgenol* 1995;164:1265-70.
15. Glowinsky A, Adam G, Brücker A, Neuerburg J, van Vaals JJ, Günther RW. Catheter visualization using locally induced,

actively controlled field inhomogeneities. *Magn Reson Med* 1997;38:253-8.

16. Atalar E, Kraitchman DL, Carkhuff B, Lesho J, Ocali O, Solaiyappan M, Guttman MA, Charles HK Jr. Catheter-tracking FOV MR fluoroscopy. *Magn Reson Med* 1998;40:865-72.
17. Baker KB, Tkach JA, Nyenhuis JA, Phillips M, Shellock FG, Gonzalez-Martinez J, Rezai AR. Evaluation of specific absorption rate as a dosimeter of MRI-related implant heating. *J of Magn Reson Imaging* 2004;20:315-20.
18. Rezai AR, Finelli D, Nyenhuis JA, Hrdlicka G, Tkach J, Sharan A, Rugieri P, Stypulkowski PH, Shellock FG. Neurostimulation systems for deep brain stimulation: *in vitro* evaluation of magnetic resonance imaging-related heating at 1.5 Tesla. *J Magn Reson Imaging* 2002;15:241-50.
19. Roguin A, Zviman MM, Meininger GR, Rodrigues ER, Dickfeld TM, Bluemke DA, Lardo A, Berger RD, Calkins H, Halperin HR. Modern pacemaker and implantable cardioverter/defibrillator systems can be magnetic resonance imaging safe: *in vitro* and *in vivo* assessment of safety and function at 1.5 T. *Circulation* 2004;110:475-82.
20. Irnich W, Irnich B, Bartsch C, Stertmann WA, Gufler H, Weiler G. Do we need pacemakers resistant to magnetic resonance imaging? *Europace* 2005;7:353-65.
21. Food and Drug Administration. Center for Devices and Radiological Health *MR Product Reporting Program*. Available from: http://www.fda.gov/cdrh/mdr/; last visited 14/05/2007.
22. Martin ET, Coman JA, Shellock FG, Pulling CC, Fair R, Jenkins K. Magnetic resonance imaging and cardiac pacemaker safety at 1.5-Tesla. *J Am Coll Cardiol* 2004;43:1315-24.
23. American Society for Testing and Material (ASTM) Designation: F2182-02a. *Standard test method for measurement of radio frequency induced heating near passive implants during magnetic resonance imaging*. West Conshohocken, PA: ASTM; 2004.
24. Wickersheim KA, Sun MH. Fluoroptic® thermometry. *Med Electronics* 1987 Feb;84-91.
25. Shellock FG. Thermal responses in human subjects exposed to magnetic resonance imaging. *NY Acad Sci* 1992;649:260-72.
26. Blouin LT, Marcus FI, Lampe L. Assessment of effects of a radiofrequency field and thermistor location in an electrode catheter on the accuracy of temperature measurement. *Pacing Clin Electrophysiol* 1991;14(Part I):807-13.
27. Shellock FG, Schaefer DJ, Kanal E. Physiologic responses to an MR imaging performed at a specific absorption rate of 6.0 W/kg1. *Radiology* 1994;192:865-8.
28. Shellock FG, Shields CL Jr. Radiofrequency energy-induced heating of bovine articular cartilage using a bipolar radiofrequency electrode. *Am J Sports Med* 2000;28:720-4.
29. Dinerman JL, Berger RD, Calkins H. Temperature monitoring during radiofrequency ablation. *J Cardiovasc Electrophysiol* 1996;7:163-73.
30. Institute of Electrical and Electronics Engineers. C95.3-1991: *Recommended practice for measurements and computations with respect to human exposure to radiofrequency electromagnetic fields, 100 kHz to 300 GHz*. New York: IEEE; 1991.
31. Mattei E, Triventi M, Calcagnini G, Censi F, Kainz W, Bassen HI, Bartolini P. Temperature and SAR measurement errors in the evaluation of metallic linear structures heating during MRI using fluoroptic probes. *Phys Med Biol* 2007;52:1633-46.
32. Duru F, Luechinger R, Scheidegger MB, Luscher TF, Boesiger P, Candinas R. Pacing in magnetic resonance imaging environment: clinical and technical considerations on compatibility. *Eur Heart J* 2001;22:113-24.
33. Nitz WR, Oppelt A, Renz W, Manke C, Lenhart M, Link J. On the heating of linear conductive structure as guide wires and Catheters in interventional MRI. *J Magn Reson Imaging* 2001;13:105-14.
34. Ruggera PS, Witters DM, von Maltzahn G, Bassen HI. *In vitro* assessment of tissue heating near metallic medical implants by exposure to pulsed radio frequency diathermy *Phys Med Biol* 2003;48:2919-28.